Critical Magnetic Fields of Superconducting SnTe

R. A. HEIN
Naval Research Laboratory, Washington, D. C. 20390
AND
P. H. E. MEIJER
The Catholic University of America, Washington, D. C. 20017
(Received 18 March 1968; revised manuscript received 20 October 1968)

Upper critical magnetic fields $H_{c2}(T)$ of five samples of superconducting SnTe possessing different values of the nominal carrier concentration P^* have been measured as a function of the temperature. Lower critical field data $H_{c1}(T)$ were also obtained on four of these samples. Values of P^* vary from a low of 7.5×10^{20} per cm^3 to a high of 20.0×10^{20} per cm^3. The superconducting transition temperatures T_0 increase with increasing P^* from a low of 0.034°K to a high of 0.214°K. Values for $H_{c2}(T)$ were obtained from the magnetic field dependence of both ac and dc magnetic susceptibility data. Values for $H_{c1}(T)$ were obtained from measurements of the magnetic moment as a function of magnetic field. The observed values of $H_{c1}(T)$ were rather small, being of the order of 10^{-1} Oe. Application of the Ginsburg-Landau-Abikosov-Gor'kov (GLAG) formulas to the critical magnetic field data allows one to calculate values for the Ginsburg-Landau parameter κ. Values of κ are found to increase with increasing values of P^* and range from a low of 3.9 to a high of 6.1. Application of the Goodman-Gor'kov equation to the normal-state parameters of this material lead to values which are about 25% higher than the above values. The agreement between the observed T_0's and the theoretical predictions of Allen and Cohen is reasonably good.

I. INTRODUCTION

CURRENT interest in the occurrence of superconductivity in degenerate semiconductors stems from the theoretical predictions of Cohen that suitable degenerate many-valley semiconductors should exhibit superconductivity in a low but *experimentally attainable* temperature region[1] and the nearly simultaneous discovery[2] that the degenerate many-valley semiconductor GeTe is a superconductor at temperatures below 0.4°K. The subsequent discoveries that the degenerate semiconductors $SrTiO_3$[3] and SnTe[4] were also superconductors at temperatures between 0.02 and 0.5°K promulgated the theoretical concepts of Cohen into a state of relative prominence.

$SrTiO_3$ is the most extensively studied superconducting semiconductor; zero-field transition temperature T_0,[5] critical magnetic fields, and specific heats[6] have been studied as functions of the carrier concentration. Studies of the superconducting penetration depth[7] and pressure effects[8] on T_0 have also been performed. In the case of GeTe, superconducting tunneling data,[9] specific-heat data,[10] and the variation of T_0 and critical magnetic fields with carrier concentration[11] have been published. Specific-heat data,[12] tunneling data,[13] and the variation of T_0 with carrier concentration[4,14] for SnTe have also been published.

Critical magnetic field data obtained for $SrTiO_3$ and GeTe allow one to classify these materials as type-II superconductors with values for the Ginsburg-Landau parameter[15] κ, which depend upon the carrier concentration. Values for κ in these materials range from a low of 2 to a high of 9.

The present investigation was undertaken to obtain critical magnetic field data on the samples of SnTe for which T_0 had been previously reported,[4] Since the original manuscript describing the current work was submitted, the report of Hulm *et al.*[14] appeared, which reports the observation of superconductivity in self-doped samples of SnTe for carrier concentrations as low as 4.6×10^{20} per cm^3. This result is in contrast to the earlier report[4] that a sample with a carrier concentration of 7.5×10^{20} per cm^3 was not superconducting at temperatures above 0.03°K. The data of Hulm *et al.*[14] indicate that a sample with this latter carrier concentration should possess a T_0 of about 0.06°K. In view of this, we have reinvestigated the lower carrier concen-

[1] M. L. Cohen, Rev. Mod. Phys. **36**, 240 (1964); Phys. Rev. **134**, A511 (1964).
[2] R. A. Hein, J. W. Gibson, R. Mazelsky, R. Miller, and J. K. Hulm, Phys. Rev. Letters **12**, 320 (1964). See remarks by J. K. Hulm which followed the paper by Cohen, Ref. 1, p. 242.
[3] J. F. Schooley, W. R. Hosler, and M. L. Cohen, Phys. Rev. Letters **12**, 474 (1964).
[4] R. A. Hein, J. W. Gibson, R. S. Allgaier, B. B. Houston, Jr., R. Mazelsky, and R. C. Miller, in *Proceedings of the Ninth International Conference on Low-Temperature Physics*, edited by J. G. Daunt, D. O. Edwards, F. J. Millford, and M. Yaqub (Plenum Press, Inc., New York, 1965).
[5] J. F. Schooley, W. R. Hosler, E. Ambler, J. F. Becker, M. L. Cohen, and C. S. Koonce, Phys. Rev. Letters **14**, 305 (1965).
[6] E. Ambler, J. K. Colwell, W. R. Hosler, and J. F. Schooley, Phys. Rev. **148**, 280 (1966).
[7] J. F. Schooley and W. R. Thurber, J. Phys. Soc. Japan Suppl. **21**, 639 (1967).
[8] E. R. Pfeiffer and J. F. Schooley, Phys. Rev. Letters **19**, 783 (1967).
[9] P. J. Stiles, L. Esaki, and J. F. Schooley, Phys. Letters **23**, 206 (1966).
[10] L. Finegold, Phys. Rev. Letters **13**, 233 (1964).
[11] R. A. Hein, J. W. Gibson, R. L. Falge, Jr., R. Mazelsky, R. C. Miller, and J. K. Hulm, J. Phys. Soc. Japan Suppl. **21**, 643 (1967).
[12] L. Finegold, J. K. Hulm, R. Mazelsky, N. E. Phillips, and B. B. Triplett, Physica **210**, 129 (1966).
[13] L. Esaki and P. J. Stiles, Phys. Rev. Letters **16**, 1108 (1966).
[14] J. K. Hulm, C. K. Jones, D. W. Dies, H. A. Fairbanks, and P. A. Lawless, Phys. Rev. **169**, 388 (1968).
[15] L. Ginsburg and L. D. Landau, Zh. Eksperim. i Teor. Fiz. **20**, 1064 (1952).

tration samples for the occurrence of superconductivity using an ac inductance method in place of the earlier dc method. We have revised the manuscript to include a discussion of the dependence of T_0 upon carrier concentration.

Section II contains a description of the samples and experimental techniques employed in this study. Section III presents the zero magnetic field data and subsequent discussion in light of the recent theory of Allen and Cohen.[16] In Sec. IV the various critical magnetic field data are presented and discussed in Sec. V in terms of the BCS theory[17] and various modifications of the Ginsburg-Landau-Abikosov-Gor'kov (GLAG) theory.[18] Section VI contains the summary of the findings of this investigation.

II. EXPERIMENTAL DETAILS

A. Samples

1. Fabrication

SnTe is one of the group–IV-VI semiconducting compounds. In general, the tellurides of the IV*A* elements do not form stoichiometric compounds. The nonstoichiometric alloys are denoted as $A_{1-x}Te_1$, where *A* is either Ge, Pb, or Sn. Limits on the magnitude of x are governed by the respective phase fields, since only single-phase samples are meaningful in the current investigation. For $Sn_{1-x}Te_1$, which crystallize in the NaCl-type structure, the single-phase region exists for $0<x\leq 0.04$.[19]

Critical magnetic field data contained in this report were obtained on samples of $Sn_{1-x}Te_1$ supplied by Houston, and Allgaier of the U. S. Naval Ordnance Laboratory. These samples were in general polycrystalline, although some were single crystals, and were grown from a melt using the Czochralski pulling technique. Either a stoichiometric melt or a slightly Te-rich melt, 50.4 at. % Te, was employed. The highest P^* sample was an as-pulled sample which was annealed in a Te-rich atmosphere for 1000 h and air quenched. The intermediate P^* values were obtained by melting the appropriate amounts of Sn and Te in a 6-mm-diam quartz tube and water quenched. The samples were then annealed in a sealed tube for 100 h.

2. Carrier Density

Tin telluride is always deficient in tin,[20] since the composition is of the form $Sn_{1-x}Te_1$, where $x>0$, and belongs to the class of materials known as self-doping semiconducting compounds. This terminology arises from the fact that each Sn vacancy contributes a number of holes to the valence band; thus SnTe is a *p*-type semiconductor.

The nominal carrier concentration P^* present in these samples was determined by Allgaier and Houston from measurements of the Hall voltage at 77°K. For the samples involved in this study the Hall coefficient becomes temperature-independent below about 100°K. Thus P^*(77°K) is a good measure of the number of holes which the sample possess at liquid-helium temperatures.

B. Cryogenic Aspects

Temperatures below 1°K were produced by the magnetic cooling technique. The physical principles upon which this process is based are well documented.[21]

The arrangement used for the cooling of three samples in a given experiment is depicted in Fig. 1. Potassium chrome alum is crystallized about one end of a bundle of from 600 to 900 uninsulated 0.005-in.-diam copper wires. The solid salt is then shaped by hand to form a cylindrical "salt pill". The samples to be investigated, denoted as S-1, S-2, and S-3, are placed in intimate thermal contact with the paramagnetic salt "pill," denoted as P. This is accomplished by enmeshing the samples inside the bundle of copper wires (which form the thermal link L) by the use of G.E. Adhesive No. 7031 and nylon thread. At the far end of the thermal link L is a 470-Ω, ¼-W Speer carbon resistor CR. A manganin wire heater H is wound around the thermal link as shown in Fig. 1.

This assembly of salt "pill," samples, carbon resistor, and heater is suspended from the brass top plate TP by means of a nylon thread. The necessary electrical leads for the carbon resistor and heater are wrapped around the salt "pill" and then thermally anchored to the top plate by means of a copper post and G.E. Adhesive No. 7031. From the copper post the leads are passed up the pumping line PL and brought out of the vacuum system through a seal at room temperature.

Two mutual inductance coil systems are positioned as shown in Fig. 1. The larger diameter coil system C-1 consists of a primary and two secondary windings and is used to measure the incremental magnetic susceptibility of the salt "pill." The smaller diameter coil system C-2 of Fig. 1 consists of a primary and four secondary coils. This system is used to measure the incremental magnetic susceptibility of the three samples under investigation. Magnetic susceptibility measurements are performed with both ac and dc mutual inductance bridges.

---

[16] P. Allen and M. L. Cohen, Phys. Rev. **177**, 704 (1969).

[17] J. Bardeen, L. N. Cooper, and J. R. Schrieffer, Phys. Rev. **108**, 1175 (1957).

[18] Reference 15 plus the following: (a) A. A. Abrikosov, Dokl. Akad. Nauk SSSR **86**, 489 (1952); (b) A. A. Abrikosov, Zh. Eksperim. i Teor. Fiz. **32**, 1342 (1957) [English transl.: Soviet Phys.—JETP **5**, 1147 (1957)]; (c) L. P. Gor'kov, Zh. Eksperim. i Teor. Fiz. **36**, 1918 (1959) [English transl.: Soviet Phys.—JETP **9**, 1364 (1959)]; (d) L. P. Gor'kov, Zh. Eksperim. i Teor. Fiz. **37**, 1407 (1959) [English transl.: Soviet Phys.—JETP **10**, 593 (1960)].

[19] B. B. Houston, Jr. (private communication).

[20] A. Sagar and R. C. Miller, in *Proceedings of the International Conference on the Physics of Semiconductors, Exeter* (The Institute of Physics and the Physical Society, London, 1962), p. 653.

[21] D. de Klerk, in *Encyclopedia of Physics*, edited by S. Flügge (Springer-Verlag, Berlin, 1956), Vol. 15, pp. 38–54.

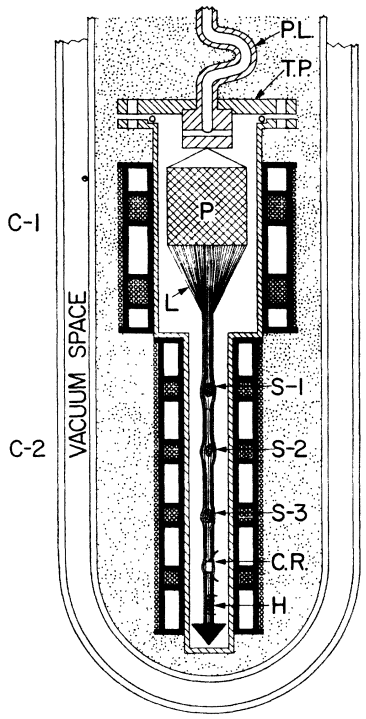

FIG. 1. A schematic of the sample and paramagnetic salt arrangement. P is the potassium chrome alum salt "pill" used for the production of the ultralow temperatures; L is the thermal link used to cool the samples to the temperature of the salt pill. This thermal link is made up of from 600 to 800 bare copper wires 0.005 in. in diameter; S denotes samples in general, with S-1, S-2, and S-3 denoting the three samples, respectively; H is a Manganin wire coil wrapped around the thermal link and serves as a heater. The coil has a resistance of approximately 300 Ω; C-1 is the mutual inductance coil system used for measuring the temperature dependence of the magnetic susceptibility of the paramagnetic salt pill; C-2 is the mutual inductance coil system used for measuring the temperature dependence of any one of the three samples; CR is a Speer 470, ¼-W carbon resistor; PL is the pumping line for the vacuum system; and TP is the brass top plate of the vacuum "can."

The entire assembly of can and coils is lowered inside a conventional glass helium Dewar system. The lower end of the Dewar is placed inside a mu-metal case in order to shield the samples from the residual magnetic field of the laboratory. Magnetic susceptibilities of the samples and salt "pill" as well as the dc electrical resistance of the carbon resistor are measured as functions of the temperature as the temperature of the helium bath is reduced from 4.2 to 1.2°K.

After completion of the 1.2°K measurements, the Dewar is removed from the mu-metal case and placed in a high-field magnet. This movement is accomplished with the aid of a hoist and trolley system.

At this point, the magnetic field is turned on and the system is isothermally magnetized. The large steady magnetic fields required for the magnetic cooling process are supplied by Naval Research Laboratory's (NRL) 4.25-in.-diam water-cooled solenoid. Fields as high as 50 000 Oe were employed in this investigation.

The carbon resistor always changes its value due to the heating associated with the magnetization of the paramagnetic salt. The helium exchange gas present in the "can" usually conducts the heat into the helium bath in about 10–15 min. The exchange gas is then pumped out, 10–20 min pumping time, and the magnetizing field is reduced to zero. The Dewar is then removed from the magnet and repositioned either in the mu-metal case or in a mu-metal–clad air-core solenoid. Magnetic susceptibility measurements performed on the salt within a few minutes after the demagnetization usually indicated that temperatures in the neighborhood of the ordering temperature of the salt were obtained, i.e., 0.01°K.

Temperatures below 1°K were determined from susceptibility measurements performed on the paramagnetic salt "pill." The carbon resistor served merely to indicate the relative rate of warming or cooling of the samples.

C. Magnetic Moment and Magnetic Susceptibility Measurements

Zero-magnetic-field transition temperatures as well as critical magnetic fields were determined magnetically. The magnetic properties of the samples which were measured in the present investigation are the incremental magnetic susceptibility χ_{inc} and magnetic moment $\mathfrak{M}$. These quantities were measured as functions of magnetic field and temperature by mutual inductance techniques.[22] Such measurements involve three magnetic fields: (1) the measuring field H_p of the primary winding of the mutual inductance; the magnitude of the measuring field was either 0.2 or 0.6 Oe in the dc techniques and as small as 0.002 Oe in the ac measurements; (2) the external magnetic field H_{ex} produced by the external solenoid; (3) the total magnetic field acting on the sample which is denoted as H_t and is the vector sum of H_p and H_{ex}.

dc magnetic susceptibility measurements were performed by a mutual inductance method described in detail elsewhere.[22] In this method a small dc current I_p is initiated through the primary winding and the deflection θ of a ballistic galvanometer connected in series with a given pair of oppositely wound secondary coils is observed. The galvanometer deflection θ is related to χ_{inc} of the sample serving as the core of the secondary coils by the relationship

$$\theta = K\chi_{\text{inc}} + \theta_0 = K(\Delta\mathfrak{M}/\Delta H) + \theta_0, \qquad (1)$$

where K and θ_0 are constants of the over-all circuitry for a given value of I_p and $\mathfrak{M}$ is the magnetic moment of the sample.

ac magnetic susceptibility measurements were also performed by a mutual inductance method using the two following procedures. (a) A lock-in amplifier and x-y recorder were used in place of the dc power supply

[22] *Encyclopedia of Physics*, edited by S. Flügge (Springer-Verlag, Berlin, 1956), pp. 71–76.

and ballistic galvanometer of the dc method. In zero applied magnetic field, the net voltage induced in the secondary coils was biased to zero. The voltage change was then recorded as a function of H_{ex} as H_{ex} was increased at a slow steady rate of 2.5 Oe per min or less. This method is readily suitable for the determination of the field at which the sample first behaves in a normal manner. (b) To obtain more detailed information concerning the ac susceptibilities of the samples the mutual inductance coils were incorporated into a Hartshorn-type bridge.[23] A two-phase lock-in amplifier served as the power supply and detector for the bridge. With this arrangement both the reactive, in-phase component χ' and the resistive, out-of-phase component χ'' of the complex ac susceptibility of the samples $\chi=\chi'+i\chi''$ were observed as functions of H_{ex}.

Using the bridge arrangement of procedure b, data were obtained in two fashions: (1) point by point and (2) "swept" dc fields. In the point-by-point method, H_{ex} is increased to some constant value and the bridge is balanced. Then H_{ex} is once again increased to a new constant value and the bridge is brought into balance once again. This continues until the bridge balance is essentially independent of H_{ex}. In the "swept" dc-field method, the bridge is balanced with the sample in the superconducting state and then H_{ex} is increased at a slow constant rate. Any unbalance in the reactive or resistive component of the bridge is automatically recorded as a function of H_{ex} upon two x-y recorders. Both methods allow one to observe essentially the magnetic field dependence of χ' and χ''.

Magnetic moment measurements were performed as a function of magnetic field by use of a method described in detail by Cochran *et al.*[24] In this technique, the primary winding of the mutual inductance serves as an external solenoid. The ballistic galvanometer is connected in series with a given pair of oppositely wound secondary coils. The current I_p is then increased from zero in a stepwise manner. Each incremental increase in I_p produces a deflection of the galvanometer θ^i. In the present study the circuitry was arranged so that 30 equal incremental steps in I_p, hence ΔH_p, could be made. A plot of

$$\sum_{i=1}^{30}[\theta^i(T)-\theta_n{}^i] \text{ versus } \sum_{i=1}^{30}\Delta H_p{}^i,$$

where $\theta^i(T)$ is the deflection observed when the sample is at a temperature $T<T_0$ and $\theta_n{}^i$ is the deflection observed when the sample is in the normal state, is simply the magnetization curve of the sample appropriate for the temperature T. This follows from Eq. (1) and the fact that in this technique $H_p=H_t$.

[23] E. Maxwell, Rev. Sci. Instr. **36**, 553 (1965).
[24] J. F. Cochran, D. E. Mapother, and R. E. Mould, Phys. Rev. **103**, 1657 (1956).

III. ZERO-MAGNETIC-FIELD DATA

The initial work[4] concerned with the dependence of T_0 upon P^* for SnTe employed a dc mutual inductance method to detect the superconducting transitions. In that study a measuring field H_p of between 0.2 and 0.6 Oe was employed depending on the size of the sample and coil system involved in the measurements. The dc magnetic susceptibility χ_{inc} of the sample with $P^*=7.5\times10^{20}/\text{cm}^3$ was observed to be temperature-independent down to the lowest temperature involved, namely, 0.03°K. In view of the recent ultralow-temperature results of Dies[14,25] we have reinvestigated the samples using a two-phase lock-in amplifier in conjunction with a Hartshorn-type bridge.[23] The use of this arrangement to measure the temperature dependence of the in-phase component χ' and the out-of-phase component χ'' of the complex ac magnetic susceptibility of the samples results in data of the type shown in Figs. 2 and 3. In this series of experiments somewhat lower temperatures were attained than in the initial work.[4] As a result of this we observed that the dc susceptibility ($H_p\approx0.6$ Oe) of the $7.5\times10^{20}/\text{cm}^3$ sample did become slightly diamagnetic at the lowest temperatures; however, the observed change in χ_{inc} was only 20% of that observed for a similarly sized sample which possessed a $P^*=10.5\times10^{20}/\text{cm}^3$. Upon switching to the ac bridge we observed the full change in χ, expected for a sample which exhibits the perfect magnetic shielding property associated with the superconducting state.

Figure 2 contains a plot of the temperature dependence of χ' and χ'' observed as the sample slowly warmed after being cooled to about 0.01°K. Note that as the sample passes from the superconducting to the normal state χ' increases in a monotonic fashion but that χ''

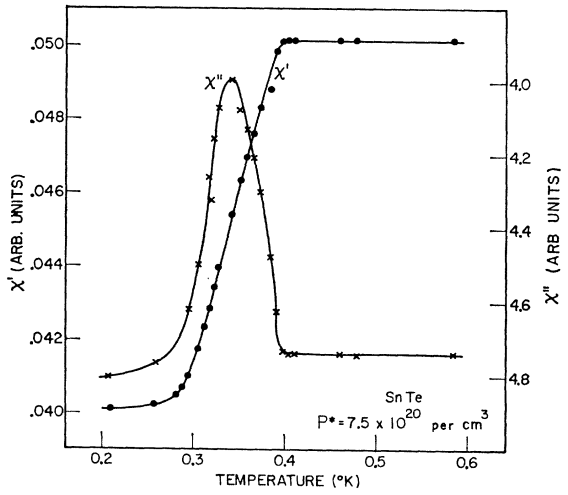

FIG. 2. The in-phase component χ' and out-of-phase component χ'' of the complex ac magnetic susceptibility of the sample with $P^*=7.5\times10^{20}/\text{cm}^3$ as functions of the absolute temperature.

[25] D. Dies, Ph.D. thesis, Duke University (unpublished).

passes through a sizable maximum. Changes in χ'' are associated with changes in the over-all losses occurring in the sample as a result of its being subjected to the ac measuring field. Figure 3 shows the temperature dependence of χ' and χ'', observed for the sample with $P^*=10.5\times10^{20}/\text{cm}^3$; dc data are also included in this figure. Data in Figs. 2 and 3 were obtained in a residual field of 0.008 Oe with an ac measuring field of 0.015 Oe at a frequency of 27 Hz.

We will digress a bit and discuss the significance which one can ascribe to a sharp ac or dc zero-field transition as deduced from measurements of the total magnetic susceptibility. A previous publication, devoted to this topic, emphasized the importance of magnetic field data and the observation of a differential paramagnetic effect (DPE).[26] Subsequent to that publication, Maxwell and Strongin[27] emphasized the importance of observing both χ' and χ'' and not simply the total ac magnetic susceptibility $\chi=\chi'+\chi''$. They

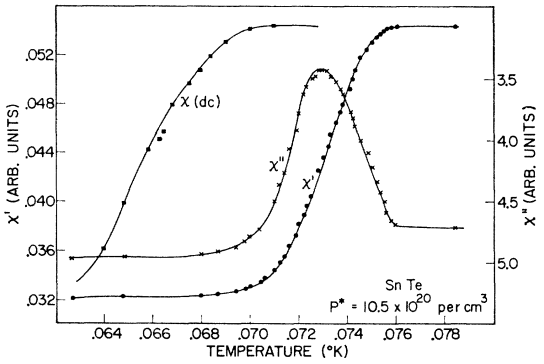

FIG. 3. The dc incremental magnetic susceptibility χ_{inc}, in-phase component χ', and out-of-phase component χ'' of the complex ac magnetic susceptibility of the sample with $P^*=10.5\times10^{20}/\text{cm}^3$ as functions of the absolute temperature.

showed that a maximum in the zero field χ''-versus-T plot is evidence for what they called "filamentary" superconductors. To emphasize this point, we show some unpublished data of Gibson and Hein in Figs. 4 and 5.

Figure 4 shows data obtained on a well-annealed sample of tin. The monotonic increase in both χ' and χ'' as the sample passes from the superconducting to the normal state is characteristic of a superconductor which possesses a reversible magnetization curve, i.e., a good Meissner effect. Figure 5 shows data obtained on a $TiCr_{1.65}$ alloy. Here, once again, χ' is monotonic but χ'' exhibits a maximum. Such behavior is characteristic of a superconductor which exhibits an irreversible magnetization curve. A maximum in χ'' of the type seen in Figs. 2, 3, and 5 is a manifestation of the fact that the sample traps some of the magnetic flux

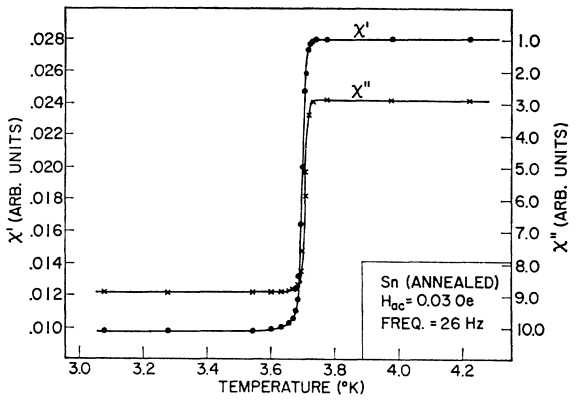

FIG. 4. The in-phase component χ' and out-of-phase component χ'' of the complex ac magnetic susceptibility of an annealed sample of tin as functions of the absolute temperature.

associated with the measuring field. One knows that as the temperature of the sample increases from some $T<T_0$, a value of the temperature is attained at which the measuring field, no matter how small, drives the sample into the intermediate or mixed state; thus if the mixed state is capable of trapping magnetic flux the loss component χ'' will reflect this as an increase in χ''. As the temperature continues to increase the sample is driven normal and χ'' takes on its normal-state value.

Figure 3 also includes a plot of the dc magnetic susceptibility χ_{inc} as a function of the temperature. These data show that the ac data yield a T_0 about 0.01°K higher than do the dc data. This is not simply the result of a larger measuring field but is related to the response of an nonideal superconductor to ac magnetic fields.[28] However, in the case of the sample with $P^*=7.5\times10^{20}/\text{cm}^3$, it is the magnitude of the dc measuring field (0.6 Oe) which prevents the observation of the full dc transition. This fact will become apparent in Sec. IV.

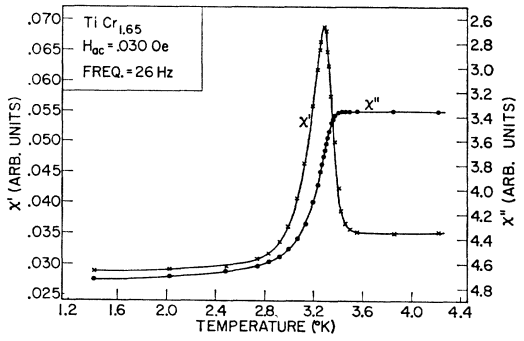

FIG. 5. The in-phase component χ' and out-of-phase component χ'' of the complex ac magnetic susceptibility of the alloy $TiCr_{1.65}$ as functions of the absolute temperature.

[26] R. A. Hein and R. L. Falge, Jr., Phys. Rev. **123**, 407 (1961).
[27] E. Maxwell and M. Strongin, Phys. Rev. Letters **10**, 212 (1963).

[28] There have been many letters and articles published dealing with this subject. The reader is referred to R. W. Rollins and J. Silcox, Phys. Rev. **155**, 404 (1967), for a fairly comprehensive bibliography.

We have included the dc data and gone through the above digression in order to emphasize two facts. (1) Data which show that χ'' passes through a maximum as the sample warms in zero applied field means that zero-field ac magnetic susceptibility data may not be representative of the superconducting properties of the bulk material. (2) Samples which exhibit a maximum in the χ'' plots will exhibit ac transitions at somewhat higher temperatures than will dc data. Specific-heat data will indicate still a lower T_0 for such materials. These facts are well known but are often overlooked.

In Fig. 6(a) we have plotted the values of T_0, obtained from the extrapolation of the critical magnetic fields (Figs. 13 and 14) to zero magnetic field, as a function of P^*. The data point for $P^*=7.5\times10^{20}$ is an average value for the midpoint of the χ' curves, Fig. 2, obtained from several different experiments. Figure 6(a) also includes the data of Hulm *et al.*[14] for the self-doped sintered samples.

The observed T_0 values taken in conjunction with the specific-heat results allow one to estimate the value of the BCS interaction parameter V. This is accomplished via the BCS result[17]

$$KT_0=1.14\langle\hbar\omega\rangle_{\text{av}}\exp[-1/N(0)V]. \quad (2)$$

V is the BCS interaction parameter, $N(0)$ is the density of electron states evaluated at the Fermi energy, and $\langle\hbar\omega\rangle$ is an average phonon energy.

Equation (2) is the result of restricting the phonon energies of importance to a region of $K\Theta_D$ of the Fermi energy.[17] In view of this it has become common practice to replace $\langle\hbar\omega\rangle$ by $\frac{3}{4}K\Theta_D$. This permits one to express Eq. (2) as

$$N(0)V=[\ln(0.855\ \Theta_D/T_0)]^{-1}. \quad (3)$$

Thus a knowledge of T_0 and Θ_D permits the evaluation of the quantity $N(0)V$.

Finegold *et al.*[12] obtained, for a sample of composition $Sn_{0.975}Te_{1.000}$, a value of (141 ± 3)°K for Θ_D. The calculated carrier concentration for a sample of this composition is $13.7\times10^{20}/cm^3$. Data of Fig. 6(a) indicate that T_0 for such a sample is 0.12°K. These values of T_0 and Θ_D in Eq. (3) lead to a value of 0.145 for the quantity $N(0)V$. Elemental metallic superconductors possess values of $N(0)V$ which range from a low of 0.155 for Ti to a high of 0.499 for Pb.[29] Thus superconducting SnTe exhibits values of $N(0)V$ which are not very different from those of metallic superconductors.

It is fairly common practice to use specific-heat data for γ, the coefficient of the linear term in the specific heats, in order to calculate an effective interaction parameter V^{eff}, defined as

$$V^{\text{eff}}=N(0)V/\gamma. \quad (4)$$

The basis for this calculation is the fact that $N(0)$ is directly proportional to γ. Thus, one finds that for $Sn_{0.975}Te_1$, $V^{\text{eff}}=0.105$. Once again we find agreement with the values reported for the metallic superconducting elements for which the range of V^{eff} is 0.013 to 0.173.

If specific-heat data were available for all of the samples, the data of Fig. 6(a) would allow one to calculate a V^{eff} for each compound. Unfortunately such data do not exist. However, if one assumes that over the small range of composition involved in this work Θ_D is approximately constant, then one can calculate $N(0)V$ for the various samples from the data of Fig. 6(a) and Eq. (3). Results of such a calculation are included in Fig. 6(b). A similar analysis of the data obtained for the sintered samples led Dies[25] to the $N(0)V$ values shown in Fig. 6(b). Both sets of T_0-versus-P^* data show that $N(0)V$ decreases with decrease in P^* but with slightly different variations.

If we assume that the ac data obtained for the sample with $P^*=7.5\times10^{20}/cm^3$ yields a T_0 of about 0.01°K larger than would suitable dc data, then $N(0)V$ for this sample would be reduced, as indicated in Fig. 6(b). Dies'[25] ultralow-temperature results and the somewhat higher temperature results of Hulm *et al.*[14] were obtained with an ac technique in which only the in-phase component was measured, so that no estimate of the degree of reversibility of the sample's magnetization curves can be given. We know that sintered samples do not exhibit as sharp a dc transition as do the grown samples[4] but the ac transitions were quite sharp.[14] A sharp ac transition is not sufficient data to allow one to conclude anything about the reversibility of the magnetization curve[26]; however, a broad dc transition is indicative of a hysteretic magnetization curve. In view of this it is not unreasonable to say that the ac data obtained on sintered samples may be indicating T_0 values in excess of the bulk transition temperature of the compound. A downward shift of the ac data of about 0.02°K would bring the two sets of data into good agreement except at the high-P^* side of Fig. 6(a).

Measuring techniques may be only part of the story as a direct comparison between sintered and grown samples clearly indicate a difference in their respective T_0-versus-P^* characteristics.[4] Thus, without results of a detailed metallurgical study one can only speculate as to the reason for this discrepancy in the T_0 data between sintered and grown samples.

At the time Hulm *et al.*[14] published their data, existing theories regarding superconducting semiconductors[1,30,31] did not permit, in general, a quantitative check between experiment and theory. Thus they analyzed their data on the basis that the $Sn_{1-x}Te_1$ compounds could be treated as metallic alloys and disregarded any band-structure complications. They based their theoretical development on the theories of Morel

[29] D. Pines, Phys. Rev. **109**, 280 (1957).

[30] J. Appel, Phys. Letters **17**, 1045 (1966).

[31] D. M. Eagles, Phys. Rev. **164**, 489 (1967).

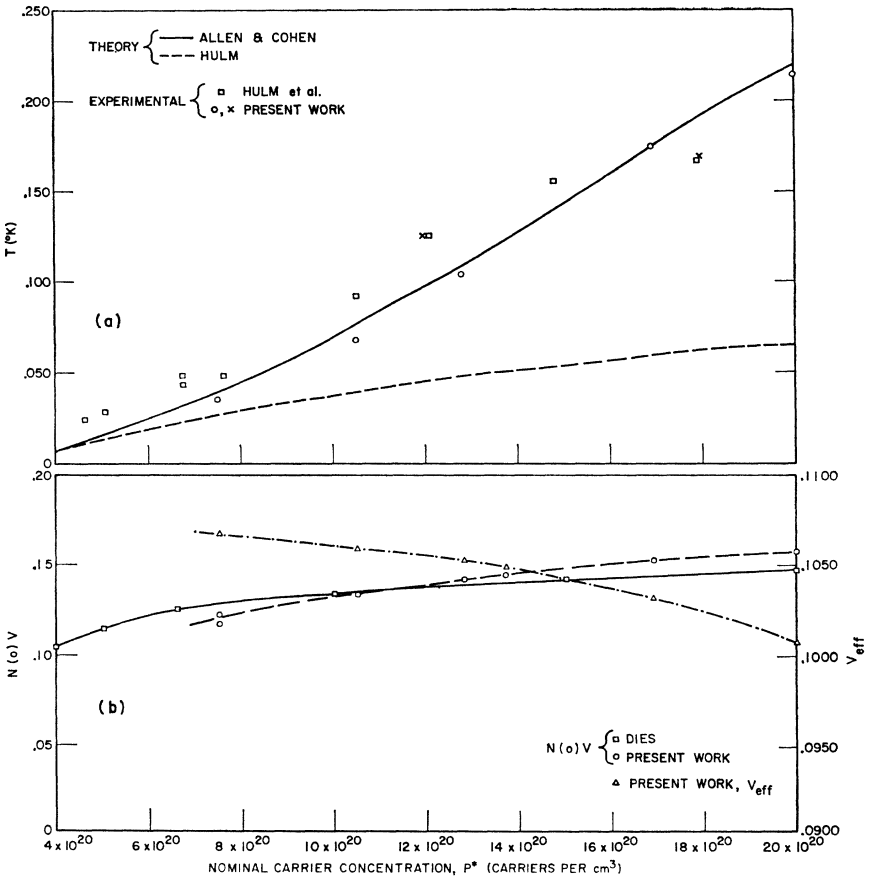

FIG. 6. (a) Zero-field transition temperature T_0 as a function of the nominal carrier concentration P^*. Experimental data points denoted by □ are those of Hulm *et al.* (Ref. 14), while those data points denoted by ○ and × are results of the present investigation. The solid curve is the theoretical dependence predicted by Allen and Cohen (Ref. 16) while the dashed curve is that of Hulm *et al.* (Ref. 14). (b) $N(0)V$ and $N(0)V/\gamma = V^{\text{eff}}$ as functions of the nominal carrier concentration P^*. Values derived by Dies (Ref. 25) are denoted by □ while values derived in the present work are denoted by ○. Values for V^{eff} are denoted by △.

and Anderson[32] and McMillian.[33] The theoretic prediction of T_0 versus P^* which results from this approach predicts values of T_0 which are too low; see Fig. 6(a).

Allen and Cohen[16] have recently considered the problem of superconductivity in SnTe from the point of view that these compounds are indeed many-valley semiconductors and have obtained a theoretical expression for T_0 as a function of P^*. A plot of their relation is included in Fig. 6(a) and one sees that the agreement is remarkably good indicating that it is indeed the phonon induced *intervalley* interactions which are important for the occurrence of superconductivity in SnTe.

As noted earlier the two sets of experimental data are in slight disagreement at the lower P^* values. Our data seem to lie about 0.02°K below that of Hulm *et al.* Normally, such agreement between samples prepared by the different methods mentioned plus the difference in the ac-versus-dc data for such nonreversible superconductors would be regarded as adequate and would deserve no further comment. However, in the present case further comments are required in that we feel that the data is suggestive of the fact that the presence of holes in a second valance band is important for the observation of superconductivity in this system. This second valence band is known to become populated[34] when P^* increases to a value above $2\times10^{20}/\text{cm}^3$. If this is the case then a plot of T_0 versus P^* should approach zero as P^* approaches $2\times10^{20}/\text{cm}^3$.

The analysis which Hulm *et al.*[14] place on their data, see Fig. 6(a), indicates that no cutoff is to be expected at that value of P^* at which the second valence band, for decreasing values of P^*, will become depleted. Their theoretical model predicts a cutoff at $P^*=4\times10^{19}/\text{cm}^3$ and they feel that their data are not inconsistent with this prediction. Our data lie somewhat below that of Hulm *et al.*[14] and are suggestive of a higher cutoff than that given above in keeping with the theory of Allen and Cohen.[16]

It is, of course, quite obvious that one may be pushing the data too far when one attempts to assign a lower cutoff in P^*. Theoretically one always is concerned with the transition of the bulk of the material characterized by the P^* value. To observe superconductivity in these low T_0 superconductors one must use small values of the measuring field; hence ac techniques

[32] P. Morel and P. W. Anderson, Phys. Rev. **125**, 1263 (1962).
[33] W. L. McMillian, Phys. Rev. **167**, 331 (1968).
[34] J. R. Burk, B. B. Houston, Jr., H. T. Savage, J. Babiskin, and P. G. Siebenmann, J. Phys. Soc. Japan Suppl. **21**, 384 (1966).

must be used in order to obtain the required sensitivity. ac transitions obtained on nonreversible superconductors *do not* yield bulk properties. One is also comparing the experimental data which deals with a nominal carrier concentration P^* while theory deals with the true number of carriers. Hence the agreement between theory[16] and experiment, which seems remarkably good, could be fortuitous. In any event we feel that the band structure of these superconductors which are degenerate semiconductors must be taken into account; for it is only those theories which take this feature into account that seem to be able to semiquantitatively fit the data.

IV. MAGNETIC FIELD DATA

A. dc Susceptibility Data

To obtain critical magnetic field data we initially measured the magnetic field dependence of the dc magnetic susceptibility χ_{inc}.

χ_{inc} data typical of all the SnTe samples studied in this manner are displayed in Fig. 7, where χ_{inc} is plotted as a function of H_{ex} for the sample with $P^*=16.9\times10^{20}/\text{cm}^3$. The significance of the notations first and second deflection are discussed in detail in an earlier publication.[26] Briefly stated, the first deflections are a measure of the forward slope of the "virgin" magnetization curve, while the second deflections, when different from the first, are a measure of the effective "slopes" of the minor hysteresis loops between the termini $H_t=H_{\text{ex}}$ and $H_t=H_{\text{ex}}+H_p$. The data of Fig. 7 tell one that (a) the magnetization curve is not reversible, (b) perfect shielding breaks down at very low values of H_{ex} ($H_{\text{ex}}\approx1$ Oe), (c) the magnetization curve possesses a large positive slope for 1 Oe$<H_{\text{ex}}<3$ Oe, (d) the forward slope of the magnetization curve is small (nearly normal behavior) for values of 5 Oe$<H_{\text{ex}}<56$ Oe, and (e) the sample behaves in a manner characteristic of the normal state at $H_{\text{ex}}=56$ Oe.

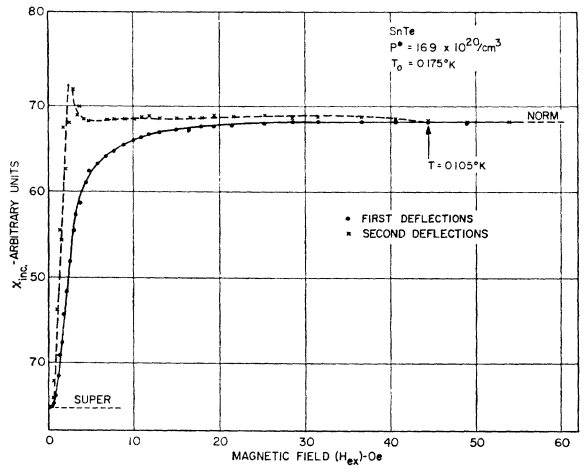

FIG. 7. Incremental magnetic susceptibility,

$$\chi_{\text{inc}}=[\Delta M/\Delta H]_{H_{\text{ex}}=0},$$

as a function of the applied magnetic field H_{ex}. $\Delta H=H_p=0.6$ Oe is the field of the primary winding. First deflections are the results of the initial application of H_p for a given H_{ex}. The field H_p is turned off and the deflection which results when H_p is reapplied is referred to as the second deflection.

Data such as these are qualitatively similar to those obtained for most superconducting alloys. The major quantitative difference is the low value of H_{ex} at which perfect shielding breaks down. To obtain more detailed information about these low penetration fields, the method of Cochran *et al.*[24] was used to measure the magnetization curves of these samples.

B. Magnetic Moment Data

Since the temperature range of interest lies below 0.3°K, there is a complication due to the fact that the samples enter the superconducting state while subjected to nonzero magnetic fields. The method of Cochran *et al.*[24] is a "summation" method; therefore, one must be certain that the magnetic moment of the sample is essentially zero at the start of the measurements. This prerequisite was met by first placing the Dewar inside a mu-metal shield (residual magnetic field $\approx10^{-2}$ Oe) and then initiating a dc current pulse through the heater H of Fig. 1. As a result of such a current pulse the temperature of the samples rises above T_0 and the frozen-in moment decreases to zero. Such thermal "purging" of the magnetic moment can be readily detected by observing the ballistic galvanometer connected in series with the appropriate pair of secondary coils. The decrease of the frozen-in moment to essentially zero produced galvanometer deflections as large as 30 mm. The behavior of the carbon resistor also indicated that the current pulse raises the temperature of the thermal link L of Fig. 1 to well above 0.3°K. The large heat capacity of the salt pill (20 g potassium chrome alum) absorbs the thermal energy associated with the current pulse and cools the samples back down to well below T_0. Since this cooling occurs in zero magnetic field no frozen-in moment should occur. A second thermal pulse always indicated no further change in magnetic moment and hence the sample is said to have been thermally purged. At this stage the summation method was used to measure the magnetization curve of the samples, on the assumption that the magnetic moment $\mathfrak{M}$ was zero when $H_{\text{ex}}=0$.

Figure 8 contains plots of

$$\sum_{i=1}^{30}\theta^i(T)-\theta^i(\text{normal})$$

in millimeters as a function of the applied magnetic field,

$$H_{\text{ex}}=\sum_{i=1}^{30}(\Delta H)^i.$$

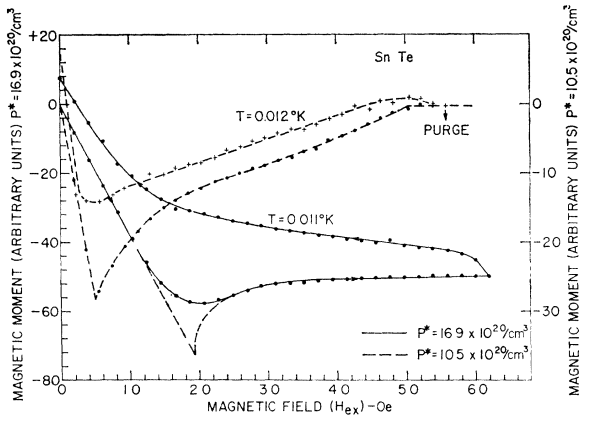

FIG. 8. Magnetic moment as a function of the applied magnetic field H_{ex} for the samples with nominal carrier concentrations P^* of $10.5\times10^{20}/cm^3$ and $16.9\times10^{20}/cm^3$.

The ordinates are thus simply the magnetic moment $\mathfrak{M}$ of the sample expressed in arbitrary units, and the data are for the samples with $P^*=10.5$ and $16.9\times10^{20}/cm^3$. These data clearly reveal the fact that the magnetic moment deviates from the linear "perfect shielding" behavior at fields below 0.5 and 1.8 Oe, respectively. In this work the value of the lower critical magnetic field $H_{c1}(T)$ will be taken as that value of the magnetic field at which an extension of the "perfect shielding" line intersects a smooth extrapolation of the $\mathfrak{M}$-versus-H curve.

A thermal purge of the sample, $P^*=10.5\times10^{20}/cm^3$, performed with $H_{ex}=5.5$ Oe produced no temperature-dependent magnetic moment. The limitation on this figure is about 5% of the maximum observed moment.

The sample with $P^*=16.9\times10^{20}/cm^3$ still possessed a considerable magnetic moment in a field of $H_{ex}=5.5$ Oe (Fig. 8). While the summation method is suitable for determining $H_{c1}(T)$ it is of limited use in the determination of the upper critical magnetic field $H_{c2}(T)$. This method is best suited for the case where $\mathfrak{M}$ is a strong function of H, which is, of course, not the case for H_{ex} in the neighborhood of H_{c2}.

C. ac Susceptibility Data

Upper critical magnetic field data can be obtained from measurements of either the dc or ac magnetic susceptibility as a function of magnetic field. The dc magnetic susceptibility data of Fig. 7 indicate that χ_{inc} of the sample behaves in a "normal-state" manner when the sample is subjected to an applied field in excess of 56 Oe. If one only wants a measure of the upper critical magnetic field, one can obtain this by using the less tedious ac mutual inductance method.

ac susceptibility data were initially obtained (see Sec. II) by first biasing to zero, in zero applied magnetic field, the net voltage induced in the secondary coils due to the ac field of the primary winding. This biasing was usually done with the sample in the superconducting state. The external magnetic field was then increased in a continuous manner and changes in the net emf induced in the secondary coils were recorded, as a function of magnetic field, by an x-y recorder. Typical data obtained in this manner for the sample with $P^*=10.5\times10^{20}/cm^3$ are presented in Fig. 9. The various curves are for different values of the magnitude of the ac primary field $|H_p|$ and different values of temperature (for fixed rate of change in H_{ex}). The shape of the emf-versus-H_{ex} curves are seen to be dependent upon the magnitude of the ac measuring field $|H_{ac}|$; this feature is an interesting study in itself and will not be discussed in this paper. With data such as these one is faced with the problem of deciding upon a reasonable and consistent experimental criterion for the upper critical magnetic field curve. For an $|H_p|$ of 0.01 Oe the upper critical field is fairly well defined. In view of this most of the ac data were obtained using an $H_p=0.01$ Oe or less. The field H_{ex} at which the sharp break in emf-versus-H_{ex} curves occurs will be denoted $H_{cu}(T)$.

To obtain more detailed information, measurements of the magnetic field dependence of χ' and χ'' were undertaken. In this series of measurements the Hartshorn-type bridge[23] was balanced with the sample in the superconducting state and the unbalance in χ' and χ'' were observed as a function of the applied magnetic field H_{ex}.

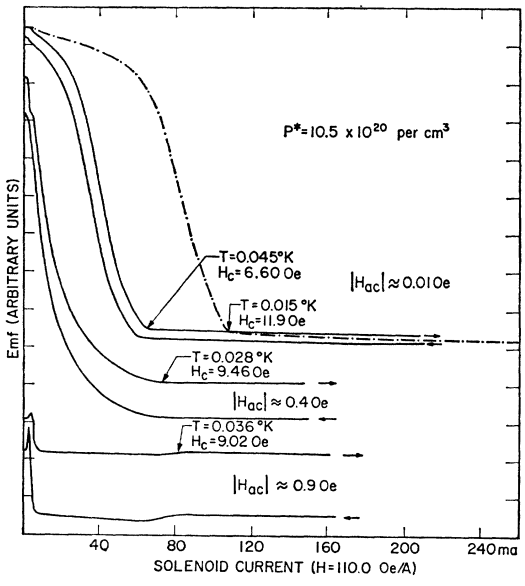

FIG. 9. Unbalanced emf of the secondary coils as a function of the applied magnetic field H_{ex}. Data were obtained by the "swept" dc field technique (Sec. II C) for various values of temperature and magnitudes of the ac measuring fields. The gain of the recorder was increased between the recording of the increasing and decreasing curves for $H_{ac}=0.9$ Oe.

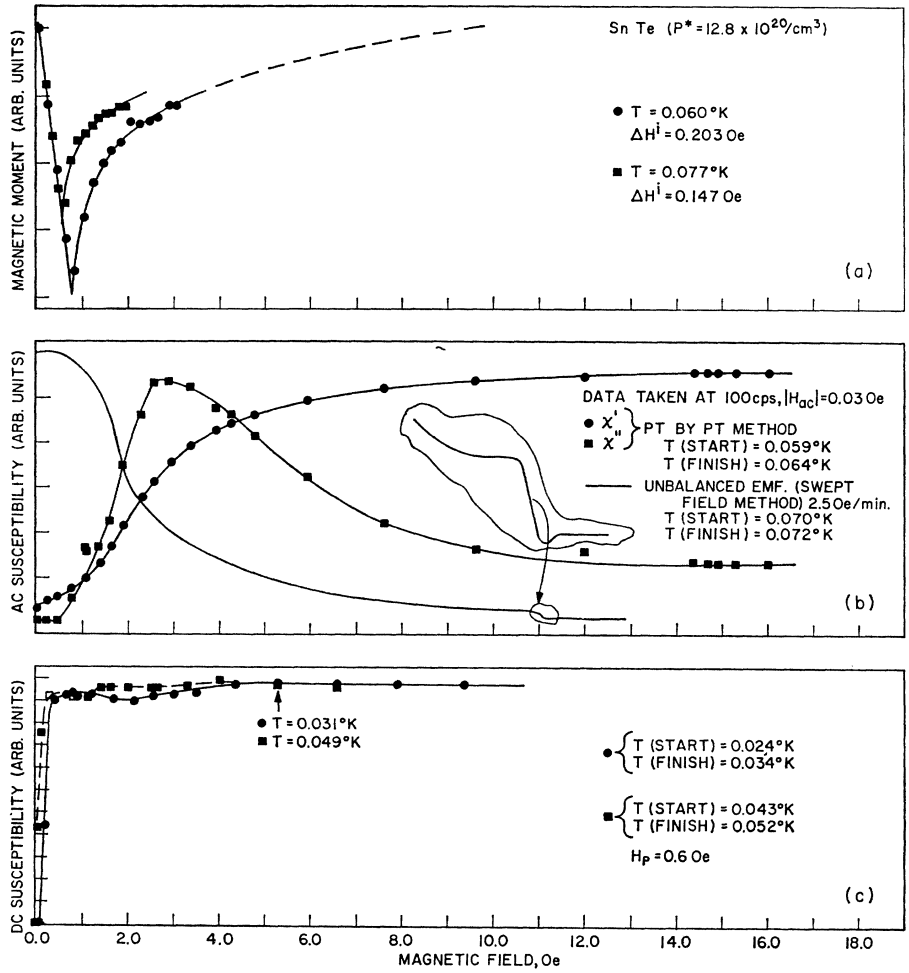

FIG. 10. (a) Magnetic moment as a function of applied magnetic field for two values of the temperature. These data as well as the data of parts (b) and (c) are for the sample with $P^* = 12.8 \times 10^{20}/\text{cm}^3$. (b) χ', χ'', and the unbalanced emf of the secondary coils as a function of applied magnetic field. χ' and χ'' data were obtained by the point-by-point technique while the unbalanced emf data were obtained by the "swept" dc field technique. The insert shows a portion of the return trace with a sensitivity of ten times that used for the increasing field data. (c) Incremental magnetic susceptibility (second deflections only) as a function of applied magnetic field for two values of the temperature.

Figure 10 presents a comparison of the various types of data obtained for the sample with $P^* = 12.8 \times 10^{20}/\text{cm}^3$. Figure 10(a) contains plots of $\mathfrak{M}$ as a function of H_{ex} for two values of the temperature. Figure 10(b) presents χ' and χ'' as functions of H_{ex}. These data were obtained by the point-by-point method (Sec. II). Figure 10(b) also includes a trace of the unbalanced emf of the secondary coils as a function of H_{ex}. This latter trace was obtained by the "swept" dc field technique. With the exception of the data obtained for the sample with $P^* = 10.5 \times 10^{20}/\text{cm}^3$ traces obtained with the "swept" field method intersect the H_{ex} axis with relatively sharp angles, as can be seen in Fig. 10(b). This small sudden change in the unbalanced emf just as the sample becomes fully normal is due to changes in the χ'' component of the magnetic susceptibility. This fact is suggested by the point-by-point data in Fig. 10(b) and clearly indicated by data of the type presented in Fig. 11. There is also a smaller less obvious effect in the χ' traces which occur at approximately the same value of H_{ex}. This small sudden drop in the χ'' component is taken as a measure of the upper critical magnetic field of the sample, $H_{cu}(T)$.

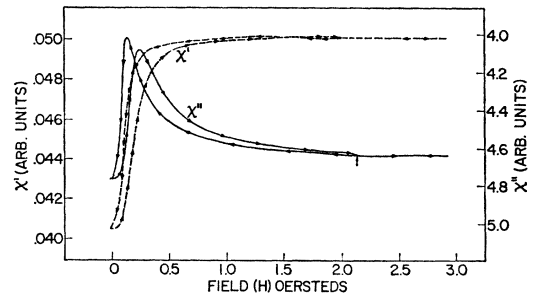

FIG. 11. In-phase component χ' and out-of-phase component χ'' of the complex ac magnetic susceptibility of the sample with $P^* = 7.5 \times 10^{20}/\text{cm}^3$ as a function of the applied magnetic field H_{ex}. Data were obtained by the swept dc field technique (Sec. II C).

Magnetic susceptibility data obtained with the dc mutual inductance method are presented in Fig. 10(c). These data are essentially second-deflection data, see Fig. 2, and were obtained using a dc measuring field H_p of 0.6 Oe. The susceptibility is seen to depart from the perfect magnetic shielding state when H_{ex} is about

0.2 Oe, or when the total field is 0.8 Oe. The magnetic moment data, Fig. 10(a), indicates that the magnetic moment begins to depart from the perfect shielding line when H_{ex} is about 0.8 Oe, so that the two sets of data are consistent.

Note that the midpoint of the dc transition bears no simple relationship to the slope of the magnetization curve. This is a consequence of the fact that these "second" deflections are reflecting the behavior of the minor hysteresis loops and are not a measure of the slope of the magnetization curve. One also sees that there is a good deal of uncertainty in experimentally defining, from such dc data, that value of H_{ex} at which the sample first returns to its normal state.

ac and dc susceptibility data yield consistent results for $H_{cu}(T)$ for the larger two P^* samples. In the case of the lower P^* samples the ac data indicated values of $H_{cu}(T)$ as much as a factor of 3 higher than the dc values for the samples for which dc data could be obtained. This behavior suggests that these samples possess "high-field" magnetization curves such that the hysteresis is large compared to the ac measuring field $\sim$0.01 Oe but small compared to the dc measuring field (0.6 Oe).

As mentioned earlier, in Sec. III, dc susceptibility measurements did not allow us to classify the sample with $P^*=7.5\times10^{20}/\text{cm}^3$ as a superconductor, but the ac susceptibility measurements did allow us to assign a T_0 for this sample (Fig. 4). We also obtained magnetic field data for this sample, which clearly shows that the magnitude of H_p was too large in the dc measurements to allow the perfect shielding aspects to be observed. Figure 11 is a plot of χ' and χ'' as a function of magnetic field for the sample under discussion; note that when $H_{ex}=0.6$, χ' is almost through its transition; thus, the dc data for $\Delta\mathfrak{M}/\Delta H$ with $\Delta H=H_p=0.6$ Oe is much less than the full diamagnetic shielding value. It is obvious from data such as these that $H_{c1}(T)$ must be less than 0.1 Oe.

D. Superconducting Surface Sheath Considerations

The interpretation of the magnetic response of a superconductor to the application of small ac magnetic fields has been the subject of numerous reports[28] and has become complicated due to the existence of a "superconducting surface sheath."[35] For an infinite superconducting cylinder in a longitudinal magnetic field, this surface sheath exists up to a critical field, denoted as $H_{c3}(T)$, which is equal to $2.4\kappa(T)H_c(T)$ or $1.69H_{c2}(T)$. $\kappa(T)$ is the Ginsburg-Landau parameter[15] and $H_{c2}(T)$ is the upper critical magnetic field of the GLAG theory.[18]

The normal-state ac skin depth at 27 Hz for a sample of SnTe whose electrical conductivity is $3.0\times10^4\,\Omega^{-1}$ cm^{-1} is calculated to be 5.7 cm. Thus, in the normal state ac magnetic flux of this frequency couples with the entire volume of the sample. The superconducting penetration depth of a sample possessing 10^{21} carriers/cm^3 is assumed to be of the order of 10^{-4} cm, or about 100 times as large as that observed in metals.[7] Whenever one uses an ac method to determine the superconducting properties of a bulk sample, he assumes that the properties of the "effective" depth to which the ac magnetic field penetrates are the same as that of the bulk material. This statement is true for dc induction methods as well.

If the surface superconducting sheath state exists, then the ac data will not reflect bulk critical magnetic fields but will yield information only about the critical magnetic fields associated with the sheath, hence $H_{c3}(T)$. It appears that it has become common practice[28] to interpret ac data obtained on nonideal samples, those which exhibit magnetic hysteresis, in terms of the surface sheath concept. The data are then used to derive values for $H_{c3}(T)$.

Strongin and co-workers[36,37] interpret the value of H_{ex} at which χ'' attains its maximum values as $H_{c3}(T)$. Malseed[38] and Doidge *et al.*[39] regard the value of H_{ex} at which χ' and χ'' depart from their normal-state values as a measure of $H_{c3}(T)$. The data presented in Fig. 10(b) indicate that values of $H_{c3}(T)$ derived on the basis of the above two criteria differ by a factor of 4. Van Englen[40] has demonstrated that the value of H_{ex} at which χ' and χ'' first return to their normal-state values is a function of the magnitude of the ac measuring field and can be a factor of 2.8 times larger than $H_{c2}(T)$, this latter critical magnetic field being obtained from magnetic moment measurements.

Since the peak in the χ'' curve Fig. 10(b) occurs at a value of H_{ex} for which $\mathfrak{M}\neq0$ the identification of this field as $H_{c3}(T)$ is not warranted. This fact and the additional observation that magnetic flux associated with H_{ac} penetrates into the sample when H_{ex} is about equal to $H_{c1}(T)$ indicates that the surface sheath state of St. James and de Gennes is not operative.

Additional data in support of this conclusion are presented in Fig. 12, where χ' and χ'' are shown as functions of H_{ex}. Data are presented for two orientations of H_{ex} relative to the axis of the sample. H_{ex} was produced by a Helmholtz pair of somewhat uncertain coil constant. This is of no serious consequence as the object of the experiment was to detect relative changes in $H_{cu}(T)$ with change in field orientation. The residual magnetic field or the laboratory was not shielded out in this experiment; therefore, $H_{cu}(T)=H^*(T)+H^{res}$.

[35] D. Saint-James and P.-G. de Gennes, Phys. Rev. Letters **7**, 306 (1963).

[36] M. Strongin, A. Paskin, D. G. Schweitzer, O. F. Kammerer, and P. P. Craig, Phys. Rev. Letters **12**, 442 (1964).

[37] A. Paskin, M. Strongin, P. P. Craig, and D. G. Schweitzer, Phys. Rev. **137**, A1817 (1965).

[38] G. F. S. Malseed, R. B. Nethercott, and W. A. Rachinger, Phys. Letters **22**, 551 (1966).

[39] P. R. Doidge, K. Sik-Hung, and D. R. Tilley, Phil. Mag. **13**, 795 (1966).

[40] P. P. J. Van Englen, G. T. C. Bots, and B. S. Blaisse, Phys. Letters **19**, 465 (1965).

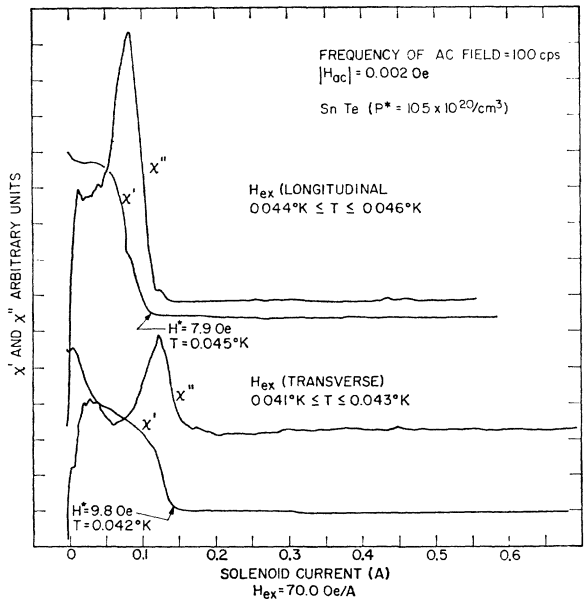

FIG. 12. χ' and χ'' data as a function of applied magnetic field for the sample with $P^* = 10.5 \times 10^{20}/\text{cm}^3$. These data were obtained by the swept dc field technique for transverse and longitudinal dc magnetic fields. Data obtained in this experiment are not included in Fig. 13.

The residual field had a longitudinal component of 1.2 Oe and a transverse component of 0.1 Oe. These values and the H^* value of Fig. 12 indicate that $H_{cu}{}^{long}$ (0.042°K) is 9.1 Oe. The slope of the $H_{cu}(T)$ curve at 0.042°K is about -23 Oe/deg; thus, $H_{cu}{}^{long}$ (0.045°K) is about 9.8 Oe. For the transverse case one sees that $H_{cu}{}^{trans}$ (0.045°K) is 9.9 Oe. Thus, to within about 1% these two fields are the same. If the surface sheath were operative, the effect of the field orientation[41] should have made $H_{cu}{}^{long}$ larger than $H_{cu}{}^{trans}$.

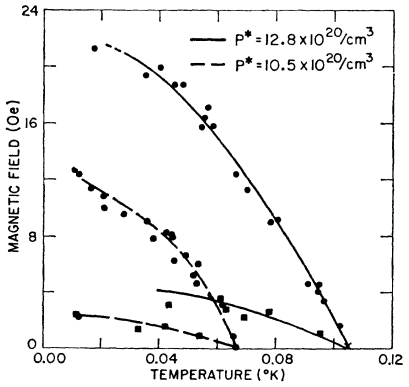

FIG. 13. Critical magnetic field data as a function of temperature for samples with $P^* = 10.5 \times 10^{20}/\text{cm}^3$ and $12.8 \times 10^{20}/\text{cm}^3$. Circles denote $H_{c2}(T)$ data while the squares denote ten times the $H_{c1}(T)$ data.

[41] P.-G. de Gennes, *Superconductivity of Metals and Alloys*, translated by P. A. Picus (W. A. Benjamin, Inc., New York, 1966).

Although $H_{cu}(T)$ is not a sensitive function of $|H_{ac}|$ or the frequency, the detailed shape of the χ curves are. These aspects of the data will not be discussed in this paper. The shape of the χ'' curves are qualitatively similar to those obtained by Maxwell and Robbins for an alloy of 4% Bi in In.[42] They identified the first (low-field) peak in χ'' with H_{c1} while the high-field peak was identified $H_{c2}(T)$.

In the analysis of the data, $H_{cu}(T)$ is considered to be a measure of $H_{c2}(T)$, not $H_{c3}(T)$. Figures 13 and 14 contain plots of ten times the $H_{c1}(T)$ deduced from the magnetization curves and $H_{cu}(T)$ values as functions of the temperature for the samples employed in this study.

Values for $H_{cu}(T)$ were obtained for the sample with $P^* = 7.5 \times 10^{20}/\text{cm}^3$ but are not plotted in either Fig. 13 or 14 because reproducible values were not obtained.

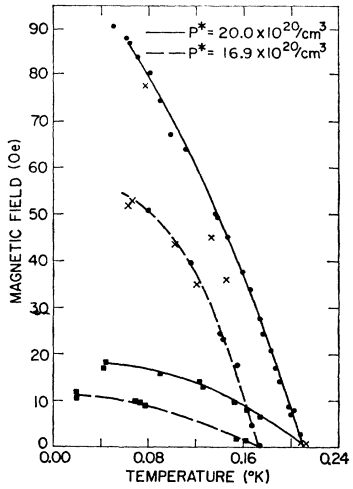

FIG. 14. Critical magnetic field data as a function of temperature for samples with $P^* = 16.9 \times 10^{20}/\text{cm}^3$ and $20.0 \times 10^{20}/\text{cm}^3$. Circles denote $H_{c2}(T)$ data while the squares denote ten times $H_{c1}(T)$ data.

For example, in the initial run a value of $H_{c2}(0.015°\text{K}) = 2.09$ Oe was obtained. The system was stored at dry-ice temperatures and a subsequent run yielded a value $H_{c2}(0.015°\text{K}) = 3.85$ Oe. Upon disassembling the system the sample was observed to be fractured into several pieces. It is not known when the cracking of the sample occurred. In a given run self-consistent data for $H_{c2}(T)$ were obtained from several demagnetizations, i.e., $H_{c2}(0.019°\text{K}) = 1.55$ Oe, $H_{c2}(0.021°\text{K}) = 1.43$ Oe; however, the subsequent run always yielded larger values, namely, $H_{c2}(0.17°\text{K}) = 2.75$ Oe and $H_{c2}(0.020°\text{K}) = 1.86$ Oe. The larger P^* samples always yielded consistent results regardless of the number of runs. We did not pursue the precise determination of the $H_{c2}(T)$-versus-T curves for the sample with $P^* = 7.5 \times 10^{20}/\text{cm}^3$.

[42] E. Maxwell and W. P. Robbins, Phys. Letters **19**, 629 (1966).

V. DISCUSSION OF CRITICAL FIELD DATA

A. Critical Magnetic Fields and κ Values

The scientific literature is rich with both experimental and theoretical works dealing with the magnetic properties of type-II superconductors. Current concepts concerning this class of materials stem from the phenomenological equations of Ginsburg and Landau,[15] the explicit solutions of these equations by Abrikosov,[18a,18b] and the extensions of these solutions by Gor'kov.[18c,18d] The expressions which result from the above group of papers are referred to as the GLAG theory.

From a measurement of T_0 and knowledge of one normal-state parameter, one can calculate values for the critical magnetic fields by use of the BCS relation

$$0.17H_c(0)^2/T_0^2=\gamma\,, \tag{5}$$

where $H_c(0)$ is the thermodynamical critical magnetic field at the absolute zero of temperature, T_0 is the superconducting transition temperature in zero applied magnetic field, and γ is the coefficient of the linear term in the normal-state specific heat in erg/cc deg^2.

Using the value due to Finegold *et al.*[12] of 1.38 mJ/mole deg^2 for γ and a T_0 value from Fig. 6(a) of 0.12°K, the above relationship yields a value of $H_c(0)$ of 5.5 Oe for the sample with $P^*=13.7\times10^{20}$. With the assumption that γ varies as $(P^*)^{1/3}$, the measured T_0 values when substituted in Eq. (5) lead to estimates of $H_c(0)$ for the other samples as listed in Table I.

The initial evidence for type-II superconductivity in these SnTe samples was the result obtained in the dc mutual inductance measurements. However, specific-heat data of Finegold *et al.*[12] allow one to derive a value for the Ginsburg-Landau parameter κ from measured normal-state parameters. This is accomplished by use of the Gor'kov-Goodman expression[43]

$$\kappa(T_0)=\kappa_0(T_0)+\kappa_l(T_0)\,, \tag{6}$$

where $\kappa_0(T_0)$ is an "intrinsic" parameter of the pure material and $\kappa_l(T_0)$ is a parameter of the alloy which is due to a mean-free-path effect. In the case of alloys $\kappa_0(T_0)\ll\kappa_l(T_0)$ and $\kappa_l(T_0)$ is given by

$$\kappa_l(T_0)=7.5\times10^3\gamma^{1/2}\rho\,, \tag{7}$$

where γ is the coefficient of the linear term in the specific heat, in units of erg/cc deg^2, and ρ is the normal-state resistivity in Ω cm.

The value due to Finegold *et al.*[12] of 1.38 mJ/mole deg^2 and a molar volume of 38.1 cc/mole, leads to a value for γ of 362 erg/cc deg^2. Using this value and a value of $3.8\times10^{-5}\,\Omega$ cm for ρ^{20} in Eq. (7) leads to a value for κ_l of 5.4. Since κ_0 is a positive quantity usually much smaller than κ_l for alloys, one sees that the Ginsburg-Landau parameter for this sample is $\kappa=5.4$, a value which clearly places this sample in the class of type-II superconductors.

The fact that these superconducting semiconductors belong to the class of type-II superconductors is also qualitatively consistent with the theoretical ideas of of Cohen.[1] He pointed out that if these materials do indeed become superconductors they will be type-II superconductors. His reason for this statement lies in the fact that such compounds will have short mean free paths (small effective coherence length) and due to the small number of carriers, when compared to those present in metallic superconductors, they should possess large penetration depths. The ratio of the penetration depth to the coherence length is a measure of the Ginsburg-Landau parameter κ, which for these compounds should be considerably greater than 0.7. Hence, type-II superconductivity should be observed.

The assumption that γ varies as $(P^*)^{1/3}$ in conjunction with the experimental values[20] for ρ leads to the κ values [Eq. (7)] for the other samples which are presented in Table I.

Using the $\kappa(T_0)$ and $H_c(0)$ values just deduced and a result of the GLAG theory, namely,

$$H_{c2}(0)=1.77\kappa H_c(0)\,, \tag{8}$$

lead to the values of $H_{c2}(0)$ presented in Table II. The agreement between these predicted values and the

TABLE I. Theoretically predicted values for $H_c(0)$ and κ_l based on measured T_0 values and one measured value for γ.

P^* (10^{20}/cm^3)	ρ ($10^{-5}\,\Omega$ cm)	$\gamma^{1/2}$ (erg/cc deg^2)	κ_l [Eq. (7)]	T_0 (°K)	$H_c(0)$ (calculated) (Oe)
20.0	4.8	20.2[a]	7.3	0.214	10.5
16.9	4.4	19.7[a]	6.5	0.174	8.3
13.7[b]	3.8	19.0	5.4	0.120	5.5
12.8	3.6	18.8[a]	5.1	0.104	4.7
10.5	3.3	18.2[a]	4.5	0.068	3.0
7.5	2.9	17.2[a]	3.7	0.034	1.4
				0.024	1.0

[a] Calculated on assumption $\gamma\sim(\rho^*)^{1/3}$.
[b] Calculated value.

[43] B. B. Goodman, Phys. Letters **6**, 597 (1961).

TABLE II. Theoretical and experimental values of several superconducting parameters.

		Calculated					Experimental					
P^* (10^{20}/cm^3)	$\kappa_l(T_0)$	$H_c(0)$ (Oe)	$H_{c1}(0)$ (Oe)	$H_{c2}(0)$ (Oe)	$-(dH_{c2}/dT)_{T_0}$ [Eq. (14)] (Oe/deg)	$-(dH_{c2}/dT)_{T_0}$ [Eq. (13)] (Oe/deg)	$H_{c1}(0)$ (Oe)	$H_{c2}(0)$ (Oe)	$-(dH_{c2}/dT)_{T_0}$	γ [Eq. (13)] (erg/cc deg^2)	$\kappa(T_0)$ GLAG	$\kappa(T_0)$ Maki
20.0	7.3	10.5	2.1	136	1037	872[a]	1.9	90	850	386	6.1	5.6
16.9	6.5	8.3	1.8	96	904	782[a]	1.2	60	800	406	5.6	4.1
12.8	5.1	4.7	1.1	42	674	517[a]	0.7	22	405	214	3.9	3.7
10.5	4.5	3.0	0.7	24	579	568[a]	0.5	13	420	181	4.4	4.2
7.5	3.7	1.4	0.4	9.2	264	130(?)	not	~5(?)	b	b	b	b
		1.0	0.3	6.5			measured					

[a] Experimentally determined κ values (GLAG) were employed.
[b] Insufficient data.

experimentally determined values (Figs. 13 and 14), while not exact, is still very gratifying (see Table II).

The GLAG theory presents $\kappa(T)$ as functions of the ratios $H_{c2}(T)/H_c(T)$ and $H_{c1}(T)/H_c(T)$. That is,

$$H_{c2}(T)=\sqrt{2}\kappa(T)H_c(T), \tag{9}$$

$$H_{c1}(T)=[\ln\kappa(T)+0.08]H_c(T)/\sqrt{2}\kappa(T). \tag{10}$$

For type-II superconductors $H_c(T)$ is not a directly observable parameter. One can obtain values of $\kappa(T)$ from measurements of $H_{c2}(T)$ and $H_{c1}(T)$ by forming the ratio

$$H_{c2}(T)/H_{c1}(T)=2\kappa^2(T)/[\ln\kappa(T)+0.08] \tag{11}$$

and solving this equation for $\kappa(T)$ by graphical means.

Equation (11) will always possess two roots for κ; one root will lie near the value of unity the other root will be considerably greater than unity. The specific-heat data as well as an evaluation of the area under the magnetization curve possible, in only a few cases in the present work, lead to values of κ which indicate that the lower root of Eq. (11) is to be discarded. Table II lists the values of $\kappa(T_0)$ obtained by a smooth extrapolation of the $\kappa(T)$ values indicated by the larger root of Eq. (11).

So far only the basic results of the GLAG theory have been used. Maki[44] has solved the Ginsburg-Landau equations for the case of alloys where the mean free path of the electrons is shorter than the coherence length. Using Maki's theoretical expressions, one can form the ratio

$$H_{c2}(T)/H_{c1}(T)=2\kappa_1(T)\kappa_3(T)/\ln\kappa_3(T), \tag{12}$$

where $\kappa_1(T)$ and $\kappa_3(T)$ are temperature-dependent parameters given as graphical functions of $\kappa(T_0)$. Values of $\kappa(T_0)$ obtained by graphical solutions of Eq. (12) are also listed in Table II.

A comparison between the κ values obtained from the GLAG and Maki formulas with those predicted from the normal-state parameters, Eq. (7), indicate that the latter values are as much as 30% too high. In view of the approximations made in the application of the Goodman-Gor'kov equation, the agreement is felt to be encouraging.

[44] K. Maki, Physics 1, 21 (1964); 1, 201(E) (1964); 1, 127 (1964).

One final remark regarding the κ values. The Goodman-Gor'kov relation, Eq. (7), leads one to expect a decrease in κ with decreasing values of P^*. This seems to be the case except for the sample with $P^*=10.5\times10^{20}$/cm^3. For the samples with the lower P^* values, the ac and dc susceptibility data yield quite different results as far as the upper critical magnetic field is concerned. If one uses the dc data as a measure of the upper critical field then the κ values for the 10.5 and 12.8×10^{20}/cm^3 samples are decreased by almost a factor of 2.[45] This feature points out the difficulties one encounters in attempting to experimentally determine, with a reasonable degree of accuracy, the critical magnetic field curves of superconductors which exhibit nonreversible magnetization curves.

B. Initial Slopes of the $H_{c2}(T)$-versus-T Curve s

If one has only a knowledge of γ and ρ he can make a rough estimate of the initial slopes of the $H_{c2}(T)$ curves as follows: For a parabolic critical magnetic field curve one has the following expression for γ in units of erg/cc deg^2:

$$\gamma=\frac{1}{8\pi}\left[\frac{dH_c}{dT}\right]^2_{T_0}=\frac{1}{16\pi\kappa^2}\left[\frac{dH_{c2}(T)}{dT}\right]^2_{T_0}, \tag{13}$$

where use has been made of the GLAG relationship, Eq. (9).

The expression for κ, Eq. (7), allows one to recast Eq. (13) as

$$[dH_{c2}(T)/dT]_{T_0}=5.3\times10^4\gamma\rho. \tag{14}$$

Using the γ and ρ values of Table I in Eq. (14) lead to the values of the initial slopes presented in Table II. Results of graphical evaluations of the initial slopes of the curves in Figs. 13 and 14 are also included in Table II. From the table one sees that the experimental values of the initial slopes are considerably smaller than the values calculated on the basis of Eq. (14). While the calculated values are a smoothly decreasing function of P^* the experimental values exhibit a sudden decrease as P^* decreases below 16.9×10^{20}/cm^3. Such behavior suggests that the density of states, hence γ, is not a smoothly decreasing function of P^*. To see this point one merely uses the experimentally derived

[45] R. A. Hein, Phys. Letters 23, 435 (1966).

values of the initial slopes and κ in Eq. (13) to solve for γ, hence for some effective density of states, $N(0)$.

Table II includes the results of such a calculation and one sees that the effective density of states drops by a factor of 2 between $P^*=16.9$ and $12.8\times10^{20}/\text{cm}^3$. This behavior is suggestive of a band-filling mechanism whereby the Fermi level for the situation where $P^*=16.9\times10^{20}/\text{cm}^3$ is such that we have holes in two or more bands but as the Fermi level rises, decrease in P^*, the lower band becomes essentially full somewhere between 16.9 and $12.8\times10^{20}/\text{cm}^3$, hence the drop in $N(0)$. This in turn decreases the intervalley scattering and as we continue to decrease P^* the intervalley scattering becomes less and less and eventually superconductivity is no longer possible. The existence of a second valance band has been proposed for SnTe but the data[34] indicated that this second band begins to be populated at a P^* of about $2\times10^{20}/\text{cm}^3$. Hence, the above analysis suggests either the presence of a third band in SnTe[46] or a region of sharp curvature in one or both bands. The fact that the calculated values for the initial slopes of the upper critical magnetic field curves are considerably larger than the observed ones is attributed to the use of the Goodman-Gor'kov values for κ in Eq. (7). Use of the κ values obtained from the measured critical magnetic fields in Eq. (13) produces calculated slopes which are in good agreement with the observed values for the larger P^* values. The persistently poor agreement between calculated and observed slopes for the lower P^* samples is felt to be the result of the assumption that γ varies as $(P^*)^{1/3}$ or it could be the result of the fact that m^* changes drastically as P^* is decreased from 16.9 to $12.8\times10^{20}/\text{cm}^3$.

The data of Figs. 13 and 14 can be used to check on the various theoretical predictions for the temperature dependence of $H_{c2}(T)$. Data for the larger P^* samples, where the ac and dc results are in good accord, fit the Gor'kov dependence somewhat better than that of Bardeen or Shapoval (see expressions given in Ref. 47). The data are not in keeping with the temperature dependence of $H_{c2}(T)[dH_{c2}/dT]_{T_0}^{-1}$ given by Werthamer *et al.*[48]; this result is not surprising since the theoretical dependence[48] results from a calculation based on a spherical Fermi surface which is not valid for SnTe.

VI. CONCLUSIONS

The occurrence of superconductivity in the SnTe system is associated with the appearance of a sufficient number of carriers, in this case holes, in a second or third valence band. The second valence band becomes populated[34] when the carrier concentration is in excess of $2\times10^{20}/\text{cm}^3$ and is believed to possess carriers of high effective mass. The T_0-versus-P^* data obtained here for grown samples indicate that P^* must be in excess of $7.5\times10^{20}/\text{cm}^3$ for the occurrence of superconductivity at $T>0.03$°K. This lower cutoff value for P^* is about a factor of 2 larger than the value of P^* at which holes begin to appear in a second valence band.[34] Thus, either there exists some threshold value for the number of holes in this second band for the occurrence of superconductivity or the observed superconductivity may be the result of holes in a still lower-lying third valence band.[46]

The deduced relationship between the appearance of holes in a second or third valence band and the occurrence of superconductivity in these IV-VI compounds lends support to the ideas of Cohen,[1] that it is indeed intervalley scattering which is important in the determination of the BCS interaction parameter V. If interband or intervalley scattering is possible, which it is if there are holes in the second band, then this intervalley scattering interaction will help overcome the repulsive Coulombic interaction and lead to a positive V, hence superconductivity.

The fact that the T_0-versus-P^* data agrees with the theoretical prediction of Allen and Cohen,[16] and disagrees with the theoretical prediction of Hulm *et al.*,[14] strongly suggests that only those theories which take into account the many-valley aspects of the band structure of these compounds are capable of explaining the data. Phonon-induced intervalley interactions seem to be the dominant mechanism[16] for superconductivity in SnTe.

Critical magnetic field data indicate that SnTe is a type-II superconductor with κ values between 3.8 and 6.1 and with κ in general increasing as P^* increases. These compounds also exhibit very low values of H_{c1}, which range in the 0.1 to 1 Oe range and which also increase with increase in P^*.

Superconductivity, when it occurs in these IV-VI semiconducting compounds GeTe, SnTe, and PbTe, seems to be due to the same cause, namely, intervalley scatterings. Thus, bulk superconductivity is not found in PbTe because one cannot as yet fabricate samples with P^* large enough so as to produce holes in the second valence band. When we learn to do this, superconductivity will most probably be observed in PbTe.

A review article dealing with the subject of superconducting semiconductors is to appear in the near future.[49]

ACKNOWLEDGMENTS

Discussions with R. S. Allgaier, B. B. Houston, Jr., J. K. Hulm, and J. F. Schooley are gratefully acknowledged. We wish to thank R. L. Falge, Jr., and J. W. Gibson for their assistance during the early phases of this work, and J. Dickert for his assistance in preparing the revised manuscript.

[46] P. J. Lin, W. Saslow, and M. L. Cohen, Solid State Commun. 5, 893 (1967).
[47] T. Kinsel, E. A. Lyton, and B. Serin, Rev. Mod. Phys. 36, 105 (1964).
[48] N. R. Werthamer, E. Helfand, and P. C. Hohenberg, Phys. Rev. 147, 295 (1966).
[49] M. L. Cohen, in *Superconductivity*, edited by R. D. Parks (Marcel Dekker, Inc., New York, 1968), Vol. 1, Chap. 12.